



OPEN ACCESS

EDITED BY

Khurshid Ahmad,
Yeungnam University, South Korea

REVIEWED BY

Melita Vidakovic,
Siniša Stanković Institute for Biological
Research, University of Belgrade, Serbia
Nemat Ali,
King Saud University, Saudi Arabia

*CORRESPONDENCE

Rongqiao He,
herq@ibp.ac.cn
Ying Liu,
yingliu@bucm.edu.cn

[†]These authors have contributed equally
to this work and share first authorship

SPECIALTY SECTION

This article was submitted to Genetics of
Common and Rare Diseases,
a section of the journal
Frontiers in Genetics

RECEIVED 31 May 2022

ACCEPTED 15 September 2022

PUBLISHED 05 October 2022

CITATION

Xi M, Zhang L, Wei Y, Li T, Qu M, Hua Q,
He R and Liu Y (2022), Effect of ribose-
glycated BSA on histone demethylation.
Front. Genet. 13:957937.
doi: 10.3389/fgene.2022.957937

COPYRIGHT

© 2022 Xi, Zhang, Wei, Li, Qu, Hua, He
and Liu. This is an open-access article
distributed under the terms of the
[Creative Commons Attribution License
\(CC BY\)](https://creativecommons.org/licenses/by/4.0/). The use, distribution or
reproduction in other forums is
permitted, provided the original
author(s) and the copyright owner(s) are
credited and that the original
publication in this journal is cited, in
accordance with accepted academic
practice. No use, distribution or
reproduction is permitted which does
not comply with these terms.

Effect of ribose-glycated BSA on histone demethylation

Mengqi Xi^{1†}, Lingyun Zhang^{1†}, Yan Wei², Ting Li³, Meihua Qu⁴,
Qian Hua¹, Rongqiao He^{2*} and Ying Liu^{1*}

¹School of Life Sciences, Beijing University of Chinese Medicine, Beijing, China, ²Institute of Biophysics, Chinese Academy of Sciences, Beijing, China, ³Bayannur Hospital, Bayannur, China, ⁴Second People's Hospital of Weifang, Weifang, Shandong, China

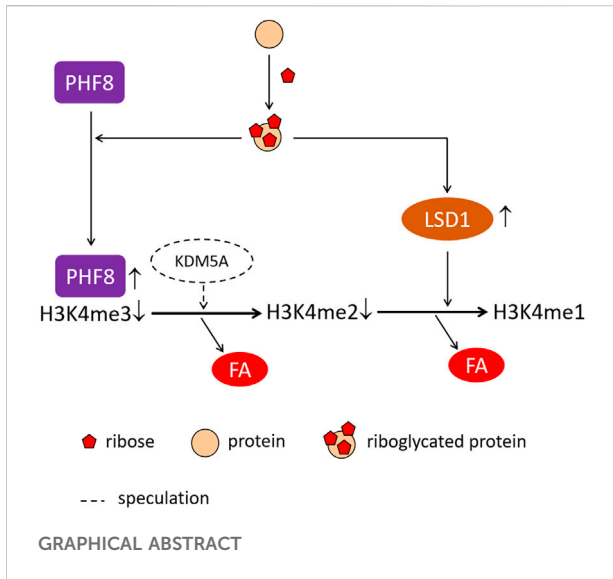
A reducing sugar reacts with the protein, resulting in advanced glycation end-products (AGEs), which have been implicated in diabetes-related complications. Recently, it has been found that both type 1 and type 2 diabetic patients suffer from not only glucose but also ribose dysmetabolism. Here, we compared the effects of ribose and glucose glycation on epigenetics, such as histone methylation and demethylation. To prepare ribose-glycated (riboglycated) proteins, we incubated 150 μ M bovine serum albumin (BSA) with 1 M ribose at different time periods, and we evaluated the samples by ELISAs, Western blot analysis, and cellular experiments. Riboglycated BSA, which was incubated with ribose for approximately 7 days, showed the strongest cytotoxicity, leading to a significant decrease in the viability of SH-SY5Y cells cultured for 24 h ($IC_{50} = 1.5 \mu$ M). A global demethylation of histone 3 (H3K4) was observed in SH-SY5Y cells accompanied with significant increases in lysine-specific demethylase-1 (LSD1) and plant homeodomain finger protein 8 (PHF8) after treatment with riboglycated BSA (1.5 μ M), but demethylation did not occur after treatment with glucose-glycated (glucoglycated) proteins or the ribose, glucose, BSA, and Tris-HCl controls. Moreover, a significant demethylation of H3K4, H3K4me3, and H3K4me2, but not H3K4me1, occurred in the presence of riboglycated proteins. A significant increase of formaldehyde was also detected in the medium of SH-SY5Y cells cultured with riboglycated BSA, further indicating the occurrence of histone demethylation. The present study provides a new insight into understanding an epigenetic mechanism of diabetes mellitus (DM) related to ribose metabolic disorders.

KEYWORDS

ribose, histone methylation, LSD1, glucose, glycation, advanced glycation end-products

Introduction

In 1815, the French chemist, M.E. Chevreul (1786–1889), discovered that the sweetness in the urine of diabetics comes from grape sugar or D-glucose (Fournier, 2011). Diabetes mellitus (DM) is considered a group of metabolic diseases characterized by hyperglycemia (high concentration of blood D-glucose), resulting from defects in insulin secretion, insulin action, or both. Ribose has been neglected until 2013 when Su



et al. (2013) first detected high levels of ribose in the urine of diabetics. After that, high blood ribose levels in both type 1 (Yu et al., 2019) and type 2 (Chen et al., 2019) diabetes have also been observed through clinical investigations. Mou et al. (2022) showed that ribose selectively glycosylates some lysine residues in bovine serum albumin (BSA) in comparison to glucose. Animal studies have also demonstrated high blood ribose levels in Zucker diabetic fatty rats (Chen et al., 2017), streptozotocin (STZ)-induced type 1 diabetes (T1D) rats (Yu et al., 2019), STZ-induced type 2 diabetes (STZ-T2D) rats (unpublished data), and Goto-Kakizaki (GK) rats (Cao et al., 2022) compared to controls. These data suggest that diabetic patients suffer from not only glucose dysmetabolism but also ribose dysmetabolism.

The reactions that lead to the formation of advanced glycation end-products (AGEs) have been known for over a hundred years since Maillard's description in 1912 (Maillard, 1912). A chronic hyperglycemic state promotes the formation of AGEs from non-enzymatic glycation of proteins, lipids, and nucleic acids in patients with DM, aggravating multiple diabetic complications (Fournier, 2011; Jud and Sourij, 2019; Khalid et al., 2022; Twarda-Clapa et al., 2022). In recent years, the relationship between glycation and epigenetics has received increasing attention (Perrone et al., 2020). Elucidation of the pathways and mechanisms of diabetic complications, resulting from hyperglycemia through epigenetic events, will aid in the prevention and treatment of diabetes.

Post-translational modifications (PTMs) of histone are powerful epigenetic mechanisms. Histone methylation can cause either relaxation or condensation of chromatin, thereby causing the activation or repression of transcription factors (Yang et al., 2020; Yamunadevi et al., 2021). The methylation process is regulated by a balance between histone-methylating and -demethylating enzymes (Chang et al., 2021). Histone demethylases are classified into two families according to their

catalytic mechanisms, namely, lysine-specific demethylases (LSDs) and Jumonji C-terminal-containing histone demethylases (JmjC demethylases) (Kim et al., 2022). The removal of methyl groups from methylated H3K4me1/2 by LSD1 (KDM1A) induces transcriptional repression, while that from methylated H3K9 induces transcriptional activation (Forneris et al., 2008). Plant homeodomain (PHD) finger protein 8 (PHF8) binds to H3K4me3-marked nucleosomes and acts as a demethylase, specific for H3K9me2 (Fortschegger et al., 2010; Liu et al., 2021).

Hyperglycemia induces a dynamic co-operativity of histone methylase and demethylase enzymes associated with gene-activating epigenetic marks (Brasacchio et al., 2009). These events may integrate and result in sustained activation of pro-inflammatory pathways, which are involved in the progression of diabetic complications (Sun et al., 2014). Histone methylation of retinal *Sod2* has an important role in the development of diabetic retinopathy and the metabolic memory phenomenon associated with its continued progression (Zhong and Kowluru, 2013). H3K4 methylation has been implicated in the dysregulation of critical genes involved in the progression of diabetic nephropathy (DN) (Yang et al., 2022). Li et al. (2021) revealed that ribose-induced nephropathy (mesangial cell injury) results from the receptor of AGE (RAGE)-dependent NF- κ B inflammation (Hong et al., 2018; Zhang et al., 2019). Targeting enzymes important for histone methylation may serve as a potential therapy to halt the development of DN and diabetic retinopathy, indicating that changes in epigenetic marks that coexist on the lysine tail during glycemia need additional investigation.

Thus far, glucose glycation (glucoglycation) has been thoroughly investigated (Brasacchio et al., 2009; Ding and Huang, 2014). However, the effects of ribose glycation (riboglycation) on genetics and epigenetics of metabolic disorders need to be clarified, especially in hyperglycemia. Histone demethylation produces formaldehyde (Shi et al., 2004), and we have observed that urine formaldehyde levels are negatively correlated with age-related cognitive abilities and education level in the elderly community (Yu et al., 2014). We have also reported a negative correlation between urine formaldehyde levels and Mini-Mental State Examination (MMSE) scores (Tong et al., 2011) as well as an association of urine formaldehyde levels with DNA de/methylation (Tong et al., 2015). Thus, formaldehyde and its metabolism may be related to de/methylation and age-related metabolic disorders (He, 2019; Li et al., 2021). In the present study, we compared the effects of ribose-glycated (riboglycated) and glucose-glycated (glucoglycated) proteins on histone de/methylation in SH-SY5Y cells. A decrease in the global methylation of H3K4 was observed followed by demethylation of H3K4me3 and H3K4me2 with a significant upregulation of LSD1 and PHF8. At the same time, formaldehyde levels increased in the culture

medium. Overall, these findings suggested that riboglycation plays a role in epigenetic diabetes-like disorders.

Materials and methods

Antibodies

The following primary antibodies were used: anti-AGEs (1:2000, 6D12, Trans Genic Inc., Japan), H3K4me1 (1:10000, ab176877, Abcam, United States), H3K4me2 (1:10000, ab32356, Abcam, United States), H3K4me3 (1:5000, ab213224, Abcam, United States), histone H3 (1:10000, ab176842, Abcam, United States), LSD1 (1:2500, 2184, Cell Signaling Technology, United States), PHF8 (1:5000, ab280887, Abcam, United States), Bax (1:5000, 50599-2-Ig, Proteintech, China), Bcl-2 (1:4000, A0208, Abclonal, China), and β -actin (1:2000, K101527P, Solarbio, China).

In vitro preparation of riboglycated BSA

BSA (Sigma, United States) was dissolved in 20 mM Tris-HCl buffer (pH 7.4) to a final concentration of 150 μ M, and it was mixed with different final concentrations (0.1, 0.5, and 1 M) of ribose (Lab Lead, China) or glucose (Ameresco, United States). As controls, 150 μ M BSA, 1 M ribose, and 1 M glucose were separately dissolved in Tris-HCl buffer. All solutions were filtered using 0.22- μ m membranes and then incubated at 37°C for 7 days without light. Aliquots were collected for measurements at different time periods from Day 1 to Day 7. The incubated products were stored at -20°C, and repeated freeze-thaw was avoided.

Western blot analysis

Protein quantification was performed using a BCA protein assay kit (Thermo Fisher, United States). The protein samples with an adjusted concentration were mixed with 5 \times SDS loading buffer and boiled for 10 min at 100°C. Proteins (3–30 μ g) (Butler et al., 2019; Abcam, 2022) were separated by 12% SDS-PAGE gels and then transferred onto PVDF membranes (Millipore, United States) at 4°C. The membranes were blocked with 5% skim milk in TBS containing 0.1% Tween-20 (TBST, pH 7.4) at room temperature for 1 h followed by incubation with primary antibodies for 2 h under the same conditions. The membranes were then washed three times with TBST and incubated with goat anti-mouse or anti-rabbit horseradish peroxidase (HRP) (1:5000, KPL, United States) at room temperature for 2 h. After three washes with TBST, the immunoreactive bands were visualized by enhanced

chemiluminescence (e-Blot Touch Imager, China), and the results were quantified using ImageJ software (<http://ImageJ.nih.gov>).

Advanced glycation end-product quantitative detection by enzyme-linked immunosorbent assay

The formation of AGEs was measured using an advanced glycation end-product (AGE) enzyme-linked immunosorbent assay (ELISA) kit (FineTest, China). In brief, the plate was washed twice with washing buffer before detection, and 50 μ l of the sample or standard was added to each well followed immediately by the addition of 50 μ l of biotin-labeled antibody. The plate was gently mixed and then incubated at 37°C for 45 min. After washing three times, 100 μ l of SABC working solution was added to each well and incubated at 37°C for 30 min. After five washes, the plate was incubated with 90 μ l of TMB substrate solution in the dark at 37°C for 15 min, and 50 μ l of stop solution was then added. The absorbance was immediately measured at 450 nm using a microplate reader (Molecular Devices, United States).

Cell culture and treatment with riboglycated protein

The human SH-SY5Y neuroblastoma cell line was obtained from the Institute of Basic Medical Sciences of the Chinese Academy of Medical Sciences (Beijing, China). The cells were cultured in Dulbecco's modified Eagle's medium (DMEM) (Gibco, United States) supplemented with 10% fetal bovine serum (FBS) (ExCell Bio, Australia), 0.1 U L⁻¹ penicillin, and 0.1 g L⁻¹ streptomycin at 37°C in a humidified chamber with 5% CO₂. The cells were grown to 80–90% confluence in 100-mm-diameter dishes and subcultured every 2 days. For all experiments, the medium was replaced with a serum-free medium before treatment with incubation products.

BSA incubated with 1 M ribose (or 1 M glucose) for 7 days was diluted with DMEM and used for the treatment of cells. As controls, 150 μ M BSA alone, 1 M ribose alone, or 1 M glucose alone was employed in the cell experiments, and 20 mM Tris-HCl buffer was used as a blank control.

Cell viability detection

Cell viability was detected using a cell counting kit-8 assay (CCK-8) (Dojindo, Japan). The SH-SY5Y cells were plated in 96-well plates at a concentration of 10⁴ cells per well. After 24 h, different concentrations of riboglycated BSA (0, 0.6, 1.2,

1.5, 1.8, 2.4, and 3 μM) were added to SH-SY5Y cells followed by measurements of cell viability after 24 h. In another experiment, 1.5 μM riboglycated BSA was added to cells 24 h after plating for different time intervals (0, 6, 12, 24, 36, 48, 60, and 72 h) followed by measurements of cell viability. After treatment, the CCK-8 reagent was added, and the plates were incubated at 37°C for 1.5 h. Under the same conditions, the cells were treated with glucoglycated BSA in addition to the ribose, glucose, BSA, and Tris-HCl controls. The absorbance was recorded at 450 nm using a SpectraMax Paradigm microplate reader (Molecular Devices, United States).

Cell apoptosis analysis by flow cytometry

The SH-SY5Y cells were plated in six-well plates at a concentration of 1.5×10^5 cells per well and cultured with 1.5 μM riboglycated BSA, 1.5 μM glucoglycated BSA, 1.5 μM BSA, 10 mM ribose, or 10 mM glucose alone for 24 h. The cells treated with Tris-HCl buffer were used as a control. Cell apoptosis was detected using an Annexin V-FITC/PI apoptosis detection kit (Beyotime, China). In brief, the cells were digested by trypsin without EDTA and washed twice with PBS. The cells (10^4) suspended with Annexin V-FITC binding solution were transferred to flow cytometry tubes and gently mixed with 4 μl of Annexin V-FITC and 10 μl of propidium iodide (PI) staining solution. The cells were then incubated at room temperature (20–25°C) for 10–20 min in the dark. Apoptotic cells were then determined by flow cytometry (BD FACSCalibur, United States), and the data were analyzed using FlowJo 7.6.1 software (TreeStar Inc., OR).

Histone extraction and global histone H3-K4 methylation detection

The experimental conditions were the same as those described previously for the cell apoptosis experiments. A global histone H3-K4 methylation assay kit (Epigentek, United States) was used to extract histones and quantify global histone H3-K4 methylation of SH-SY5Y cells according to the manufacturer's instructions.

Lysine-specific demethylase-1 quantitative detection by enzyme-linked immunosorbent assay

The experimental conditions were the same as those described previously for the cell apoptosis experiments. Lysine-specific demethylase-1 was assayed using a Human KDM1A (Lysine-specific histone demethylase 1A) ELISA Kit

(FineTest, China) according to the manufacturer's instructions.

Measurements of formaldehyde by high-performance liquid chromatography with UV detection

Formaldehyde in the medium of SH-SY5Y cells, incubated with riboglycated BSA, was quantified by high-performance liquid chromatography with UV detection (UV-HPLC). The samples of the culture medium were centrifuged (13,000 rpm, 4°C, 20 min), and the supernatants (0.4 ml) were transferred to 1.5-ml Eppendorf tubes and mixed with 0.1 ml of 10% trichloroacetic acid, 0.4 ml of acetonitrile, and 0.1 ml of 2,4-dinitrophenylhydrazine (DNPH, 0.1 g L⁻¹). The mixture was centrifuged (13,000 rpm, 4°C, 10 min) and incubated at 60°C for 30 min followed by cryogenic centrifugation to stop the reaction. The samples were filtered through 0.22- μm membranes and detected using an HPLC system (LC-20A, Japan) as described previously (Su et al., 2011).

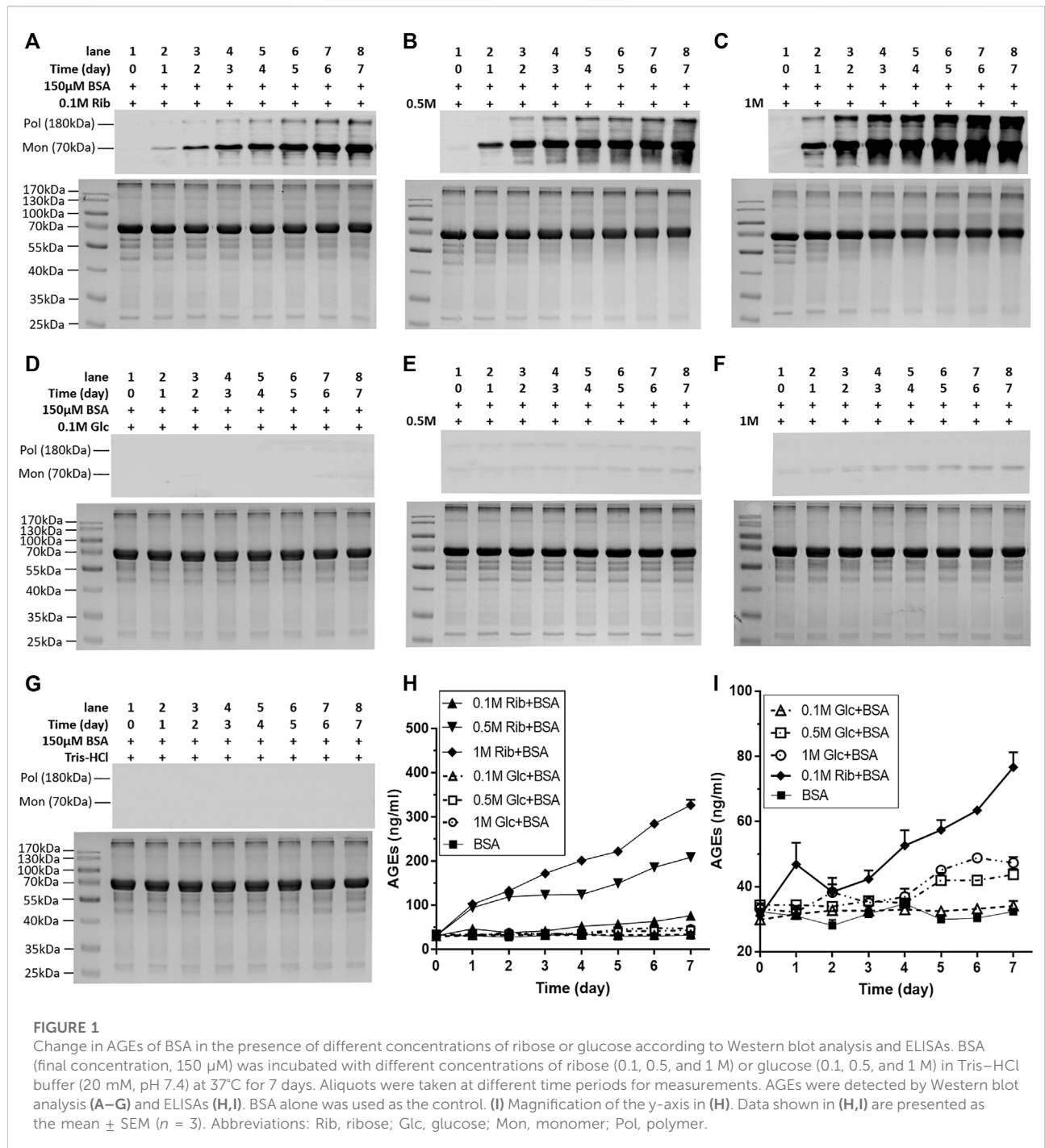
Data analysis

All data are presented as the mean \pm SEM, and all statistical analyses were performed using GraphPad Prism 7.0 software (La Jolla, United States). Statistical significance was analyzed by one-way or two-way analysis of variance (ANOVA) followed by Tukey's test for multiple comparisons. The statistical significance was set at $p < 0.05$.

Results

Riboglycation occurs more rapidly than glucoglycation

To investigate whether riboglycated protein affects histone methylation, we utilized BSA because it is commonly used as a model in glycation studies. Before determining whether changes in histone methylation induced by riboglycated proteins are different from those induced by glucoglycated proteins, we compared the BSA-glycating and AGE-producing abilities of ribose and glucose at different concentrations (Figure 1). Western blot analysis evidently exhibited that compared with those of glucose, different concentrations of ribose (0.1, 0.5, and 1 M) incubated with BSA could significantly produce many AGEs (Figures 1A–C). AGEs were visualized during the riboglycation of BSA on Day 1 and Day 2 when 0.5 and 0.1 M ribose was used, respectively. However, glucoglycation did not produce AGEs at Day 1 or Day 2, except for slight protein bands with high glucose concentration (1 M) under the



same experimental conditions (Figures 1D–F). No AGEs were observed during the incubation of BSA with Tris-HCl as the control (Figure 1G). The riboglycated BSA was prone to aggregation during incubation, resulting in polymers with a molecular mass greater than 180 kDa. A BSA monomer (approximately 70 kDa) was also observed in the SDS-PAGE and Western blot analyses. The ELISA results demonstrated that significantly more AGEs resulted from riboglycation than

glucoglycation at different concentrations for different time periods (Figure 1H).

In the kinetic study of riboglycation, we scanned the densities of protein blots at each time point and observed increases in AGEs in monomers (Figures 2A,B) and polymers (Figures 2C,D) over the incubation time. However, we did not observe a greatly increasing rate of AGEs when BSA was incubated with different concentrations of glucose (0.1, 0.5, and 1 M). We utilized Tsou’s

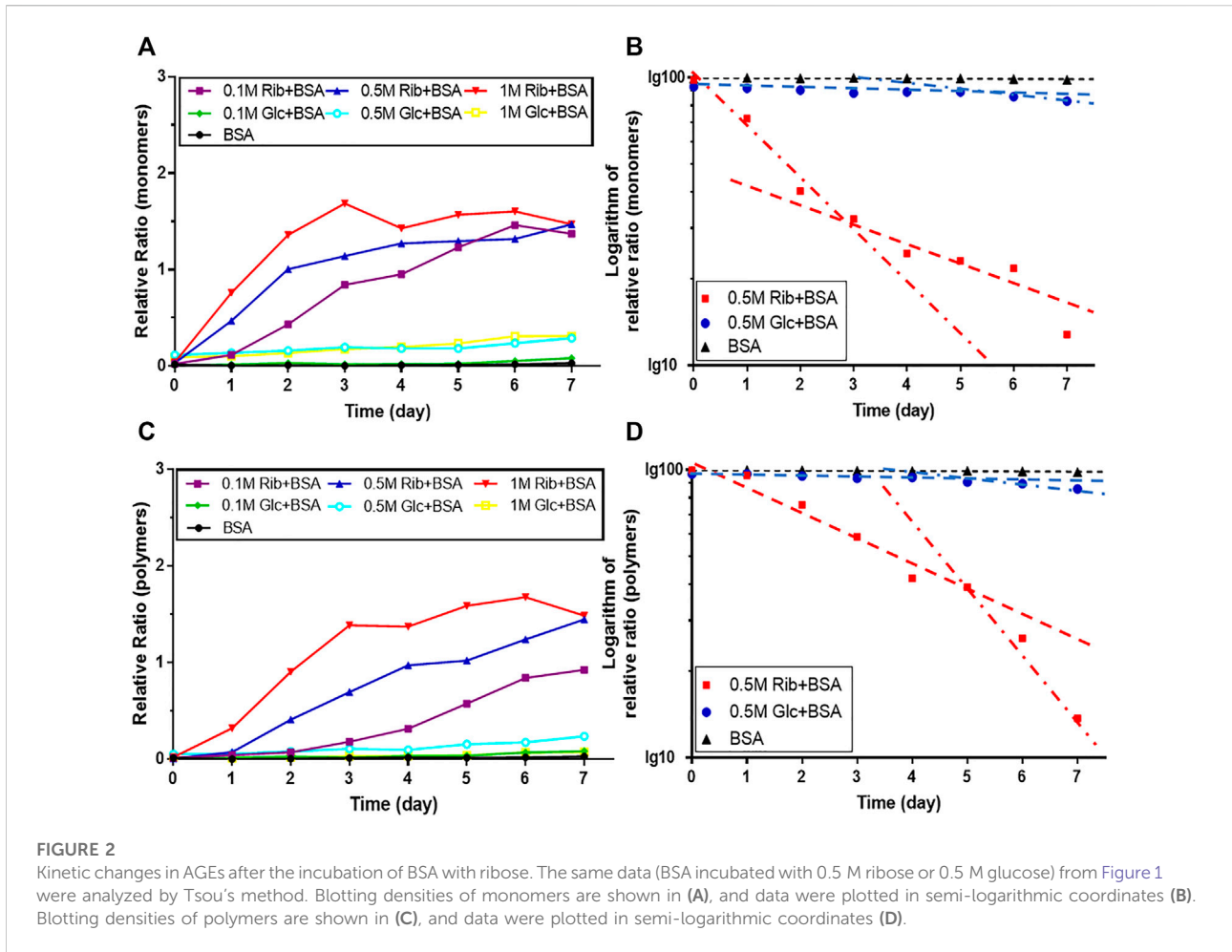


TABLE 1 First-order rate constants of BSA riboglycation and glucoglycation as calculated by Tsou's method (Tsou, 1962).

Rate constant ($\times 10^{-6} \text{ s}^{-1}$)	Polymer (180 kDa)		Monomer (70 kDa)	
	Slow	Fast	Slow	Fast
$K_{0.1R}$	0.205	2.831	1.636	6.876
$K_{0.5R}$	1.593	3.131	2.502	6.711
K_R	2.325	11.015	4.190	17.682
$K_{0.1G}$	0.079	—	0.076	—
$K_{0.5G}$	0.093	0.495	0.161	0.863
K_G	0.052	—	0.158	0.603
K_{BSA}	0.016	—	0.013	—
$K_{0.1R}/K_{0.1G}$	2.609	—	21.612	—
$K_{0.5R}/K_{0.5G}$	17.172	6.324	15.536	7.780
K_R/K_G	44.491	—	26.513	29.306

Analysis was based on the data in Figure 1. $K_{0.1R}$, $K_{0.5R}$, and K_R indicate the constants of 0.1, 0.5, and 1 M ribose incubated with BSA, respectively; $K_{0.1G}$, $K_{0.5G}$, and K_G indicate the constants of 0.1, 0.5, and 1 M glucose incubated with BSA, respectively; K_{BSA} indicates the constant of BSA alone; $K_{0.1R}/K_{0.1G}$ indicates the ratio of $K_{0.1R}$ to $K_{0.1G}$; $K_{0.5R}/K_{0.5G}$ indicates the ratio of $K_{0.5R}$ to $K_{0.5G}$; and K_R/K_G indicates the ratio of K_R to K_G .

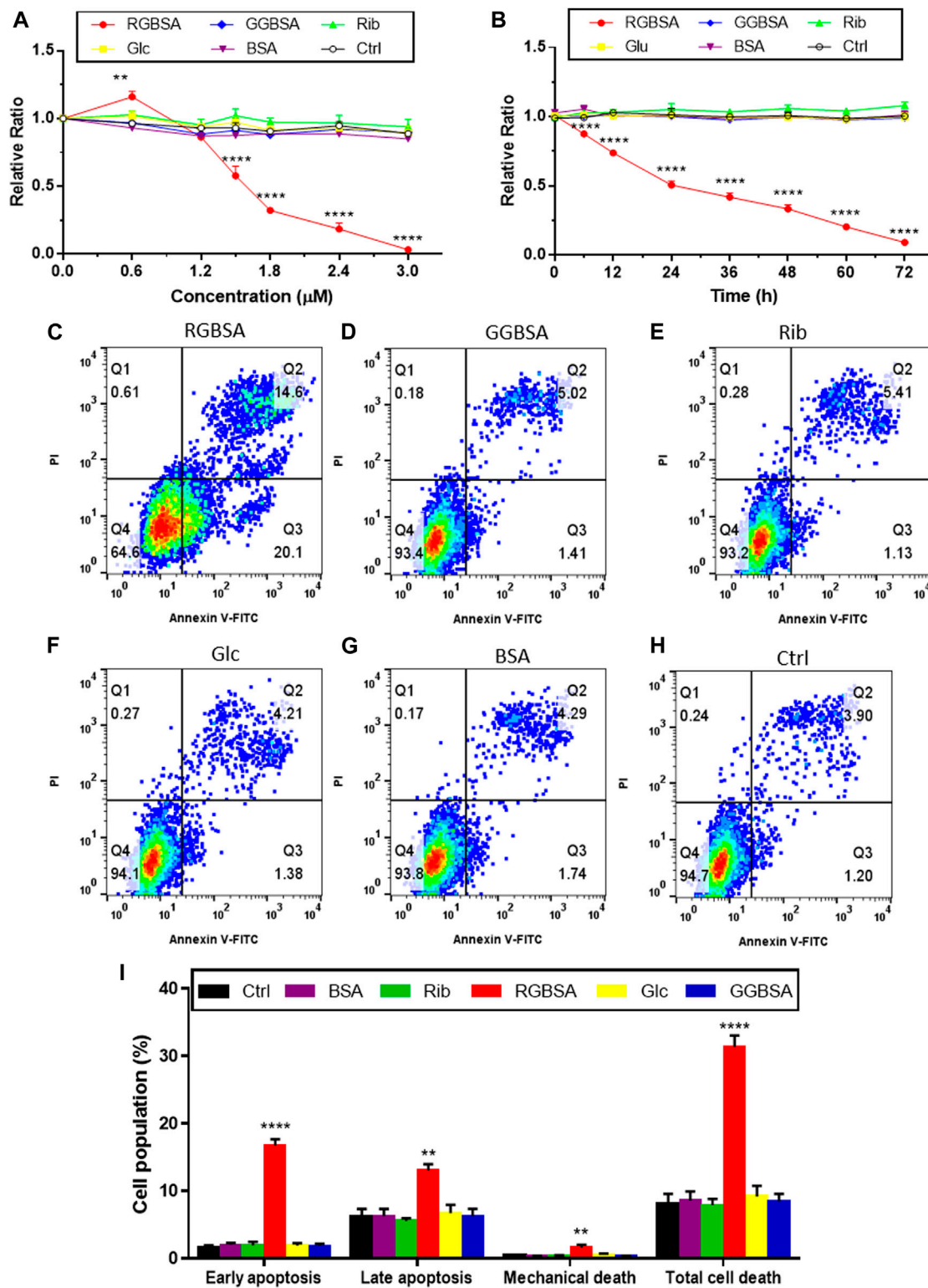


FIGURE 3

Riboglycated BSA induces SH-SY5Y cell apoptosis. Experimental conditions were the same as in Figure 1, except for SH-SY5Y cells that were incubated with different concentrations of riboglycated BSA (0, 0.6, 1.2, 1.5, 1.8, 2.4, and 3 μM) followed by the measurement of cell viability after 24 h (A) or SH-SY5Y cells that were incubated with 1.5 μM riboglycated BSA for different time periods (0, 6, 12, 24, 36, 48, 60, and 72 h) followed by the measurement of cell viability (B). Data were analyzed by two-way ANOVA and are presented as the mean \pm SEM ($n = 3$). $**p < 0.01$ and $****p < 0.0001$ compared to the control group. Flow cytometry was used to assess apoptosis of SH-SY5Y cells cultured for 24 h in the presence of 1.5 μM RGBSA (C), GGBSA (D), ribose (E), glucose (F), BSA (G), and Tris-HCl buffer (H). Percentages of apoptosis were determined by Annexin V/FITC-PI staining (I). Data were analyzed by one-way ANOVA and are presented as the mean \pm SEM ($n = 3$). $**p < 0.01$ and $****p < 0.0001$ compared to the control group. Abbreviations: RGBSA, riboglycated BSA; GGBSA, glucoglycated BSA.

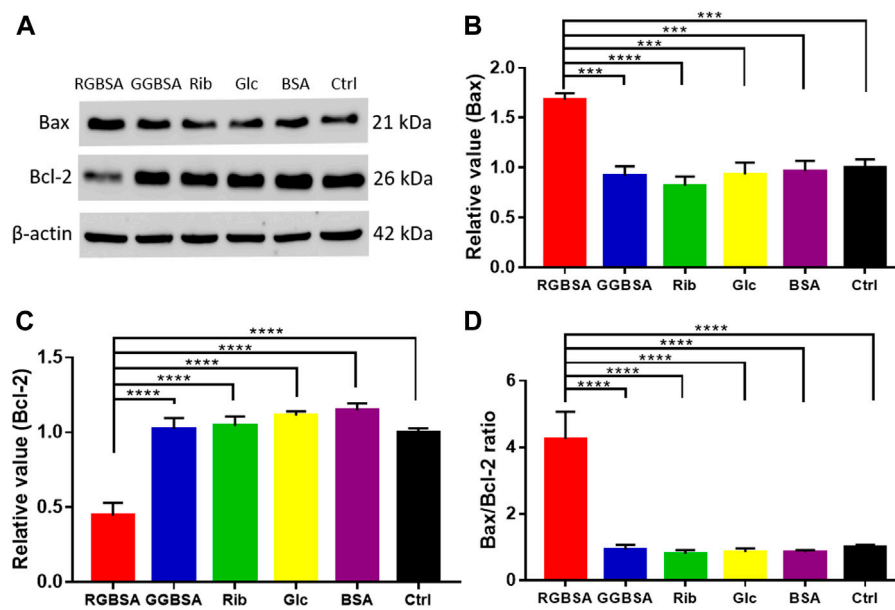


FIGURE 4

Riboglycated BSA regulates Bax and Bcl-2 proteins in SH-SY5Y cells. Experimental conditions were the same as in Figures 3C–H. The levels of Bax and Bcl-2 were determined by Western blot analysis (A). β -actin was used as the loading control. Quantification results are shown in (B,C). The control values were set at 1.0. The Bax/Bcl-2 ratios are shown in (D). All data were analyzed by one-way ANOVA and are presented as the mean \pm SEM ($n = 4$). *** $p < 0.001$ and **** $p < 0.0001$.

method (Tsou, 1962) to calculate and estimate the rate of BSA glycation of ribose. As shown in Figure 2B, the riboglycation of BSA monomers underwent a biphasic procedure (fast and slow phase), and the riboglycation of BSA polymers also underwent a biphasic procedure (slow and fast phase) (Figure 2D) with a relaxation time of approximately 1 day. The first-order rate constant of riboglycation in monomers in the fast phase for monomers ($6.71 \times 10^{-6} \text{ s}^{-1}$) was similar to that for polymers ($3.13 \times 10^{-6} \text{ s}^{-1}$), indicating that AGEs resulting from riboglycation first appear in BSA monomers and then aggregate into polymers. The comparison of the kinetic formation of AGEs showed that the first-order rate constants of riboglycation in slow and fast phases were approximately 15.5- and 7.8-fold faster than those for glucoglycation in monomers, and that they were 17.2- and 6.3-fold faster than those for glucoglycation in polymers, respectively (Table 1). Thus, these findings indicated that ribose actively participates in protein glycation and produces AGEs more rapidly than glucose at different concentrations (0.1, 0.5, and 1 M).

Riboglycated protein is more cytotoxic than glucoglycated protein

Because riboglycation is faster than glucoglycation, we next investigated whether ribose-mediated AGEs are more toxic than

glucose-mediated AGEs by evaluating SH-SY5Y cell viability after culture in the presence of riboglycated or glucoglycated BSA. Here, riboglycated BSA was the product resulting from the incubation of BSA with ribose for 7 days unless otherwise stated. As shown in Figure 3A, the viability of SH-SY5Y cells was significantly decreased as the concentration of riboglycated BSA increased, but the viability was not affected by glucoglycated BSA, ribose alone, glucose alone, or BSA alone. The IC_{50} of the inhibitory effect of riboglycated BSA on cell viability was approximately 1.5 μM . Thus, we cultured SH-SY5Y cells with riboglycated BSA at a final concentration of 1.5 μM for different time periods, and we found a significant decrease in cell viability in the presence of riboglycated BSA over time (Figure 3B). Moreover, glucoglycated BSA and the ribose, glucose, BSA, and Tris-HCl buffer controls did not significantly affect cell viability. Thus, these data indicated that riboglycated BSA is more cytotoxic than glucoglycated BSA.

Because we demonstrated that riboglycated BSA was cytotoxic, we used flow cytometry to assess the characteristics of SH-SY5Y cell death in the presence of riboglycated or glucoglycated BSA. As shown in Figure 3C, riboglycated BSA caused a significant increase in early apoptotic (Q3) SH-SY5Y cells after 24 h. In addition, there were more necrotic and late apoptotic (Q2) SH-SY5Y cells treated with riboglycated BSA compared to those treated with glucoglycated BSA (Figure 3D) and the controls (Figures 3E–H).

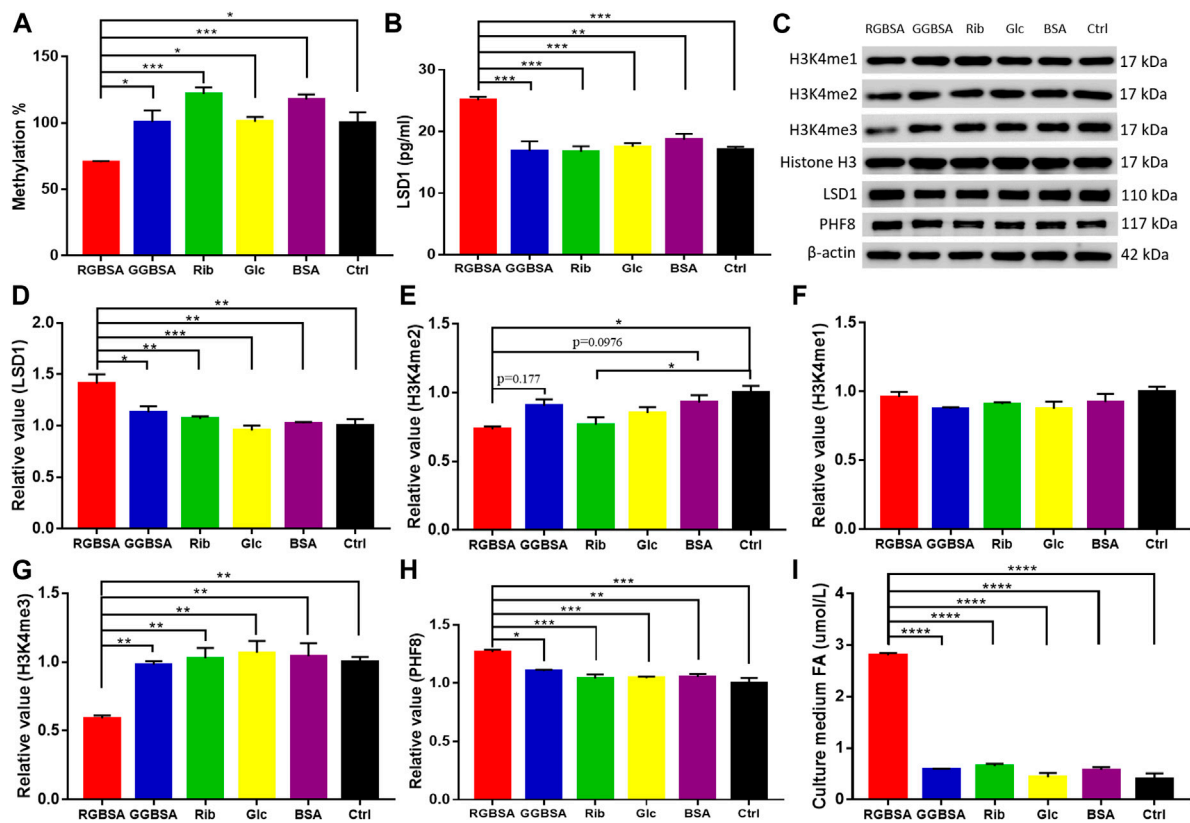


FIGURE 5

Riboglycated BSA reduces H3K4 methylation in SH-SY5Y cells. Experimental conditions were the same as in Figures 3C–H. The levels of global histone H3–K4 methylation (A) and LSD1 (B) were determined by ELISAs. The levels of H3K4me1, H3K4me2, H3K4me3, LSD1, and PHF8 in cells were determined by Western blot analysis (C). Histone H3 or β -actin was used as the loading control. Quantification results are shown in (D–H). The control values were set at 1.0. Quantitative assessment of culture medium FA levels detected by HPLC (I). All values were analyzed by one-way ANOVA and are presented as the mean \pm SEM ($n = 3$). * $p < 0.05$, ** $p < 0.01$, *** $p < 0.001$, and **** $p < 0.0001$.

To further verify that riboglycated BSA induces apoptosis (Figure 3I), we evaluated the B-cell lymphoma-2 (Bcl-2) family of genes that regulate intrinsic apoptosis, consisting of both proapoptotic and antiapoptotic members, such as Bax and Bcl-2 (Banjara et al., 2020). The Bax/Bcl-2 ratio is used to determine the survival or death of cells (Korsmeyer et al., 1993). The Western blot analysis determined the expression levels of Bax and Bcl-2 in each group (Figure 4A). The proapoptotic Bax protein was significantly upregulated, but the antiapoptotic Bcl-2 protein was inhibited in SH-SY5Y cells after treatment with riboglycated BSA compared to the control cells (Figures 4B,C). Accordingly, the Bax/Bcl-2 ratio was significantly increased by approximately 4-fold after treatment with riboglycated BSA (Figure 4D). Therefore, these findings indicated that the riboglycated protein is more capable of inducing cell apoptosis than the glucoglycated protein. However, the mechanism of how riboglycated BSA causes cell death needs further investigation.

Riboglycated bovine serum albumin increases lysine-specific demethylase-1 and plant homeodomain finger protein 8 leading to histone 3 demethylation on Lys 4

A delicate equilibrium in histone methylation and demethylation is required for proper gene regulation and maintenance of physiological metabolism (Jambhekar et al., 2019). Because changes in LSDs may lead to cellular metabolic disorders, we detected the levels of global histone methylation using ELISAs. A significant decrease in the H3–K4 methylation levels was observed in SH-SY5Y cells after incubation with riboglycated BSA compared to glucoglycated BSA ($p < 0.05$) and the ribose ($p < 0.001$), glucose ($p < 0.05$), BSA ($p < 0.001$), and Tris–HCl buffer ($p < 0.05$) controls (Figure 5A). Because LSD1 plays an important role in histone de/methylation (Leiendecker et al., 2020), we measured LSD1 protein levels

by ELISAs in SH-SY5Y cells. As shown in Figure 5B, the LSD1 levels were significantly increased in the presence of riboglycated BSA compared to glucoglycated BSA ($p < 0.001$) and the controls ($p < 0.001$ or $p < 0.01$). The Western blot analysis (Figure 5C) demonstrated that LSD1 was significantly increased after treatment with riboglycated BSA but not after treatment with glucoglycated BSA or the controls (Figure 5D).

Because histone H3 peptide methylated at lysine 4 is a substrate for LSD1, we determined the methylation levels of H3K4me1, H3K4me2, and H3K4me3 in the SH-SY5Y cells in the presence of riboglycated proteins (Figure 5C). As shown in Figure 5E, there were increased H3K4me2 demethylation levels after treatment with riboglycated BSA compared to the Tris-HCl buffer control. However, the methylation levels of H3K4me1 did not significantly decrease for all the samples under the same conditions (Figure 5F). Interestingly, the demethylation of H3K4me3 was observed in the presence of riboglycated BSA but not glucoglycated BSA or the controls (Figure 5G). The marked demethylation of H3K4me3 may suggest that other enzymes in addition to LSD1 may be involved in the modification of H3K4me3 in the presence of riboglycated proteins. For example, PHF8 demethylates H3K9me1/2, and its catalytic activity is stimulated by adjacent H3K4me3 (Feng et al., 2010). Therefore, we measured PHF8 protein levels by Western blot analysis (Figure 5C) in SH-SY5Y cells. As shown in Figure 5H, the PHF8 levels were significantly increased in the presence of riboglycated BSA compared to glucoglycated BSA ($p < 0.05$) and the controls ($p < 0.001$ or $p < 0.01$). These data suggested that LSD1 and PHF8 are both involved in H3K4 demethylation in the presence of riboglycated proteins.

Treatment with riboglycated bovine serum albumin increases formaldehyde production of SH-SY5Y cells

Because formaldehyde is a consistent metabolic product of demethylation (Kalász, 2003), we detected the formaldehyde levels in the medium of SH-SY5Y cells cultured in the presence of riboglycated BSA, glucoglycated BSA, BSA alone, ribose alone, glucose alone, and Tris-HCl alone. As shown in Figure 5I, the formaldehyde levels were higher in the medium of cells cultured with riboglycated BSA ($p < 0.001$) than the other treatments under the same experimental conditions. Thus, these data suggested that histone demethylation may act as an important source of cellular formaldehyde, which may affect the viability of SH-SY5Y cells.

Discussion

According to many researchers (Chiou et al., 1999; Zhang et al., 2020; Wang et al., 2021), employing a high concentration of reducing sugar (1 M or higher glucose) in glycation studies is a routine method to accelerate the reaction *in vitro*. However, serum protein BSA after riboglycation, but not after glucoglycation, caused high cytotoxicity. The IC_{50} , for the ability of riboglycated BSA to decrease SH-SY5Y cell viability, was 1.5 μ M. Previous clinical studies have demonstrated that blood and urine ribose levels are significantly higher in both type 1 and type 2 diabetic patients than healthy individuals (Su et al., 2013; Chen et al., 2019; Yu et al., 2019; Mou et al., 2022). In addition, blood and urine ribose concentrations are positively correlated with HbA1c and glycated serum protein, respectively. In the present study, we observed a significant increase in LSD1 and PHF8 levels as well as in H3K4me2 and H3K4me3 demethylation levels in the presence of riboglycated BSA (1.5 μ M final concentration) but not in the presence of glucoglycated BSA, suggesting that the riboglycated protein plays a role in the progression of diabetes with an epigenetic dysmetabolic disorder.

Hyperglycemia induces protein glycation, resulting in high levels of AGEs, which bind to RAGE and activate the RAGE pathway, ultimately inducing apoptosis *via* caspase 3 (Wu et al., 2018; Wu et al., 2019). The activation of the RAGE pathway leads to oxidative stress and evokes inflammatory reactions in numerous cell types and tissues, resulting in metabolic diseases (Guo et al., 2020). The present study demonstrated that riboglycation produced more AGEs at a faster rate than glucoglycation. As a monomer, we considered that riboglycated albumin binds to RAGE and triggers multiple cellular pathways, such as ROS elevation, Erk phosphorylation, NF κ B activation, and BDNF/TiKB decline (Zhang et al., 2016; Dai et al., 2019; Wu et al., 2019). These cellular pathways are associated with caspase 3 activation and promote apoptosis, indicating that riboglycated BSA induces apoptosis through a RAGE-dependent pathway (Wei et al., 2016).

As mentioned previously, riboglycated BSA induced H3K4me2 and H3K4me3 demethylation but not H3K4me1 demethylation. The present study suggested that binding of PHF8 to H3K4me3 may stimulate the demethylation of H3K4me3 by KDM5A, resulting in decreased H3K4me3. H3K4me1 may be produced from demethylation of H3K4me2. However, LSD1 is a FAD-dependent histone demethylase with homology to amine oxidases, which demethylates di- and mono-methylated K4 on histone H3 (Hou and Yu., 2010; Kooistra and Helin 2012; Fiskus et al., 2014), thereby explaining H3K4me1 accumulation in the present study. In addition, LSD1 demethylation of H3K4me2 at glucocorticoid receptor (GR)-targeted enhancers is important for GC-mediated gene transcription, suggesting a molecular mechanism for

H3K4me2 demethylation in gene activation (Clark et al., 2019). LSD1 binds to most GR-binding sites in the genome where it removes preprogrammed H3K4me2 but leaves H3K4me1 unchanged in cells. Thus, these results suggested that LSD1 and PHF8 are involved in the mechanism of riboglycated protein induction of oxidative stress.

Formaldehyde serves as a methyl donor in histone methylation (Li et al., 2021). Demethylation by both the KDM1 and JmjC demethylases oxidizes the methyl group, forming formaldehyde as a coproduct (Walport et al., 2012; Pavlenko et al., 2022). Therefore, we evaluated the formaldehyde concentration and found a significantly higher level of formaldehyde in the medium of SH-SY5Y cells cultured with riboglycated BSA than the other samples. In a complete catalytic cycle, the FAD cofactor is reduced to FADH2 and then is likely reoxidized by oxygen to produce hydrogen peroxide and formaldehyde. In general, formaldehyde is produced by more than one pathway in cells. For example, semicarbazide-sensitive amine oxidase (SSAO) catalyzes methylamine to produce formaldehyde (Yu et al., 2006), and mitochondria, as major cellular organelles, also produce formaldehyde (Xin et al., 2019). Considering that several pathways are involved in formaldehyde production, the present study suggested that H3K4 demethylation is one of the potential sources of formaldehyde.

Histone proteins are susceptible to glycation modifications due to long half-lives (for instance, 223 days in the brain) within cells and in the presence of abundant lysine and arginine residues (Commerford et al., 1982; Harmel and Fiedler., 2018; Rehman et al., 2022). Histone glycation occurs primarily on H3 and induces major chromatin changes *in vitro* and *in vivo*, and it has global ramifications on histone enzymatic PTMs and chromatin architecture as well as the assembly and stability of nucleosomes. The epigenetic impact of histone glycation was dependent on the sugar concentration and exposure time (Zheng et al., 2020a). Recent studies have suggested the interconnection of glycation with epigenetic PTMs, including histone methylation (Zheng et al., 2020b; Perrone et al., 2020), through competing sites, such as the substitution of glycation adducts for H3K4me3 and H3R8me2 (Zheng et al., 2019). As a non-enzymatic chemical modification, the occurrence of glycation is directly related to the concentration of the reactants and reaction time. However, demethylation occurs under enzyme-induced catalysis. It is well known that an enzymatic reaction is faster than a non-enzymatic reaction. Thus, further studies are required to determine whether ribose affects de/methylation due to the cross-talk between glycation and methylation of histones.

In conclusion, a low concentration (1.5 μ M) of riboglycated BSA has higher cytotoxicity in SH-SY5Y cells than glucoglycated BSA. Treatment with riboglycated BSA induces demethylation of H3K4me3 and H3K4me2, which significantly increases the LSD1 and PHF8 levels, resulting in increased formaldehyde levels in cells. In addition, other histone demethylases, such as KDM5A, may also be involved in the mechanism of riboglycated protein-induced cell toxicity. The increased formaldehyde levels

may also be attributed to other pathways in the presence of glycated BSA, thereby warranting further investigation.

Data availability statement

The original contributions presented in the study are included in the article/Supplementary Material. Further inquiries can be directed to the corresponding authors.

Author contributions

MX and LZ performed the experiments and data analysis; RH and YW designed the experiments in the manuscript; TL and MQ performed the analysis and writing; and RH, YL, and QH supervised and secured funds for the research. All authors read and approved the final manuscript.

Funding

This work was supported by the Fundamental Research Funds for the Central Universities (2020-JYB-ZDGG-051), the Beijing Municipal Science and Technology Project (Z161100000217141), the National Natural Science Foundation of China (31870840), the National Science Foundation of Inner Mongolia Autonomous Region (2021MS08040), and the Medical Science and Technology Project of Shandong Province (2019WSA07013 and 202102040075).

Conflict of interest

The authors declare that the research was conducted in the absence of any commercial or financial relationships that could be construed as a potential conflict of interest.

Publisher's note

All claims expressed in this article are solely those of the authors and do not necessarily represent those of their affiliated organizations, or those of the publisher, the editors, and the reviewers. Any product that may be evaluated in this article, or claim that may be made by its manufacturer, is not guaranteed or endorsed by the publisher.

Supplementary material

The Supplementary Material for this article can be found online at: <https://www.frontiersin.org/articles/10.3389/fgene.2022.957937/full#supplementary-material>

References

- Abcam. (2022). Histone Western blot protocol. Available at: <https://www.abcam.com/protocols/histone-western-blot-protocol> [Accessed April 28, 2022].
- Banjara, S., Suraweera, C. D., Hinds, M. G., and Kvensakul, M. (2020). The bcl-2 family: Ancient origins, conserved structures, and divergent mechanisms. *Biomolecules* 10, 128. doi:10.3390/biom10010128
- Brasacchio, D., Okabe, J., Tikellis, C., Balcerzyk, A., George, P., Baker, E. K., et al. (2009). Hyperglycemia induces a dynamic cooperativity of histone methylase and demethylase enzymes associated with gene-activating epigenetic marks that coexist on the lysine tail. *Diabetes* 58, 1229–1236. doi:10.2337/db08-1666
- Butler, T., Paul, J. W., Chan, E. C., Smith, R., and Tolosa, J. M. (2019). Misleading westens: Common quantification mistakes in western blot densitometry and proposed corrective measures. *Biomed. Res. Int.* 2019, 5214821. doi:10.1155/2019/5214821
- Cao, X., Yu, L. X., Wei, Y., Qu, M. H., and He, R. Q. (2022). Changes in ribose, AGEs and transketolase in female GK rat a type 2 diabetic model. *Prog. Biochem. Biophys.* 49, 949–952. doi:10.16476/j.pibb.2022.0161
- Chang, Y., Zhang, J., Zhang, J., Gu, Q., Zhu, W., and Han, J. (2021). Research progress of epigenetic modification in learning and memory. *Prog. Biochem. Biophys.* 48, 737–749. doi:10.16476/j.pibb.2020.0333
- Chen, X., Su, T., Chen, Y., He, Y., Liu, Y., Xu, Y., et al. (2017). D-ribose as a contributor to glycated haemoglobin. *EBioMedicine* 25, 143–153. doi:10.1016/j.ebiom.2017.10.001
- Chen, Y., Yu, L., Wang, Y., Wei, Y., Xu, Y., He, T., et al. (2019). d-Ribose contributes to the glycation of serum protein. *Biochim. Biophys. Acta. Mol. Basis Dis.* 1865, 2285–2292. doi:10.1016/j.bbdis.2019.05.005
- Chiou, Y. J., Tomer, K. B., and Smith, P. C. (1999). Effect of nonenzymatic glycation of albumin and superoxide dismutase by glucuronic acid and superphenyl acyl glucuronide on their functions *in vitro*. *Chem. Biol. Interact.* 121, 141–159. doi:10.1016/s0009-2797(99)00098-8
- Clark, E. A., Wu, F., Chen, Y., Kang, P., Kaiser, U. B., Fang, R., et al. (2019). GR and LSD1/kdm1a-targeted gene activation requires selective H3K4me2 demethylation at enhancers. *Cell Rep.* 27, 3522–3532. doi:10.1016/j.celrep.2019.05.062
- Commerford, S. L., Carsten, A. L., and Cronkite, E. P. (1982). Histone turnover within nonproliferating cells. *Proc. Natl. Acad. Sci. U. S. A.* 79, 1163–1165. doi:10.1073/pnas.79.4.1163
- Dai, J., Chen, H., and Chai, Y. (2019). Advanced glycation end products (AGEs) induce apoptosis of fibroblasts by activation of NLRP3 inflammasome via reactive oxygen species (ROS) signaling pathway. *Med. Sci. Monit.* 25, 7499–7508. doi:10.12659/MSM.915806
- Ding, G. L., and Huang, H. F. (2014). Role for tet in hyperglycemia-induced demethylation: A novel mechanism of diabetic metabolic memory. *Diabetes* 63, 2906–2908. doi:10.2337/db14-0675
- Feng, W., Yonezawa, M., Ye, J., Jenuwein, T., and Grummt, I. (2010). PHF8 activates transcription of rRNA genes through H3K4me3 binding and H3K9me1/2 demethylation. *Nat. Struct. Mol. Biol.* 17, 445–450. doi:10.1038/nsmb.1778
- Fiskus, W., Sharma, S., Shah, B., Portier, B. P., Devaraj, S. G., Liu, K., et al. (2014). Highly effective combination of LSD1 (KDM1A) antagonist and pan-histone deacetylase inhibitor against human AML cells. *Leukemia* 28, 2155–2164. doi:10.1038/leu.2014.119
- Forneris, F., Binda, C., Battaglioli, E., and Mattevi, A. (2008). LSD1: Oxidative chemistry for multifaceted functions in chromatin regulation. *Trends biochem. Sci.* 33, 181–189. doi:10.1016/j.tibs.2008.01.003
- Fortschegger, K., de Graaf, P., Outchkourov, N. S., van Schaik, F. M., Timmers, H. T., and Shiekhattar, R. (2010). PHF8 targets histone methylation and RNA polymerase II to activate transcription. *Mol. Cell. Biol.* 30, 3286–3298. doi:10.1128/MCB.01520-09
- Fournier, J. (2011). The French chemist M.-E. Chevreul (1786-1889) in several topics of public health. *Rev. Hist. Pharm.* 58, 393–412.
- Guo, Q., Li, F., Duan, Y., Wen, C., Wang, W., Zhang, L., et al. (2020). Oxidative stress, nutritional antioxidants and beyond. *Sci. China. Life Sci.* 63, 866–874. doi:10.1007/s11427-019-9591-5
- Harmel, R., and Fiedler, D. (2018). Features and regulation of non-enzymatic post-translational modifications. *Nat. Chem. Biol.* 14, 244–252. doi:10.1038/nchembio.2575
- He, R. (2019). Metabolic disorder of ribose. *Prog. Biochem. Biophys.* 46, 930. doi:10.16476/j.pibb.2019.0210
- Hong, J., Wang, X., Zhang, N., Fu, H., and Li, W. (2018). D-ribose induces nephropathy through RAGE-dependent NF- κ B inflammation. *Arch. Pharm. Res.* 41, 838–847. doi:10.1007/s12272-018-1061-z
- Hou, H., and Yu, H. (2010). Structural insights into histone lysine demethylation. *Curr. Opin. Struct. Biol.* 20, 739–748. doi:10.1016/j.sbi.2010.09.006
- Jambhekar, A., Dhall, A., and Shi, Y. (2019). Roles and regulation of histone methylation in animal development. *Nat. Rev. Mol. Cell Biol.* 20, 625–641. doi:10.1038/s41580-019-0151-1
- Jud, P., and Sourij, H. (2019). Therapeutic options to reduce advanced glycation end products in patients with diabetes mellitus: A review. *Diabetes Res. Clin. Pract.* 148, 54–63. doi:10.1016/j.diabres.2018.11.016
- Kalász, H. (2003). Biological role of formaldehyde, and cycles related to methylation, demethylation, and formaldehyde production. *Mini Rev. Med. Chem.* 3, 175–192. doi:10.2174/1389557033488187
- Khalid, M., Petroianu, G., and Adem, A. (2022). Advanced glycation end products and diabetes mellitus: Mechanisms and perspectives. *Biomolecules* 4, 542. doi:10.3390/biom12040542
- Kim, J., Lee, H., Yi, S. J., and Kim, K. (2022). Gene regulation by histone-modifying enzymes under hypoxic conditions: A focus on histone methylation and acetylation. *Exp. Mol. Med.* 54, 878–889. doi:10.1038/s12276-022-00812-1
- Kooistra, S. M., and Helin, K. (2012). Molecular mechanisms and potential functions of histone demethylases. *Nat. Rev. Mol. Cell Biol.* 13, 297–311. doi:10.1038/nrm3327
- Korsmeyer, S. J., Shutter, J. R., Veis, D. J., Merry, D. E., and Oltvai, Z. N. (1993). Bcl-2/Bax: A rheostat that regulates an anti-oxidant pathway and cell death. *Semin. Cancer Biol.* 6, 327–332.
- Leiendaeker, L., Jung, P. S., Krecioch, I., Neumann, T., Schleiffer, A., Mechtler, K., et al. (2020). LSD1 inhibition induces differentiation and cell death in Merkel cell carcinoma. *EMBO. Mol. Med.* 12, e12525. doi:10.15252/emmm.202012525
- Li, T., Wei, Y., Qu, M., Mou, L., Miao, J., Xi, M., et al. (2021). Formaldehyde and de/methylation in age-related cognitive impairment. *Genes* 12, 913. doi:10.3390/genes12060913
- Liu, Q., Pang, J., Wang, L. A., Huang, Z., Xu, J., Yang, X., et al. (2021). Histone demethylase PHF8 drives neuroendocrine prostate cancer progression by epigenetically upregulating FOXA2. *J. Pathol.* 253, 106–118. doi:10.1002/path.5557
- Maillard, L.-C. (1912). Action des acides aminés sur les sucres: Formation des melanoidines par voie méthodique. *CR Acad. Sci.* 154, 66–68.
- Mou, L., Hu, P., Cao, X., Chen, Y., Xu, Y., He, T., et al. (2022). Comparison of bovine serum albumin glycation by ribose and fructose *in vitro* and *in vivo*. *Biochim. Biophys. Acta. Mol. Basis Dis.* 1868, 166283. doi:10.1016/j.bbdis.2021.166283
- Pavlenko, E., Ruengeler, T., Engel, P., and Poepsel, S. (2022). Functions and interactions of mammalian KDM5 demethylases. *Front. Genet.* 13, 906662. doi:10.3389/fgene.2022.906662
- Perrone, A., Giovino, A., Benny, J., and Martinelli, F. (2020). Advanced glycation end products (AGEs): Biochemistry, signaling, analytical methods, and epigenetic effects. *Oxid. Med. Cell. Longev.* 2020, 3818196. doi:10.1155/2020/3818196
- Rehman, S., Aatif, M., Rafi, Z., Khan, M. Y., Shahab, U., Ahmad, S., et al. (2022). Effect of non-enzymatic glycosylation in the epigenetics of cancer. *Semin. Cancer Biol.* 83, 543–555. doi:10.1016/j.semcancer.2020.11.019
- Shi, Y., Lan, F., Matson, C., Mulligan, P., Whetstone, J. R., Cole, P. A., et al. (2004). Histone demethylation mediated by the nuclear amine oxidase homolog LSD1. *Cell* 119, 941–953. doi:10.1016/j.cell.2004.12.012
- Su, T., Wei, Y., and He, R. (2011). Assay of brain endogenous formaldehyde with 2, 4'-dinitrophenylhydrazine through UV-HPLC. *Prog. Biochem. Biophys.* 38, 1171–1177. doi:10.3724/SP.J.1206.2011.00407
- Su, T., Xin, L., He, Y., Song, Y., Li, W., Wei, Y., et al. (2013). The Abnormally high level of uric D-ribose for type-2 diabetics. *Acta Agron. Sin.* 40, 816–825. doi:10.3724/SP.J.1206.2013.00341
- Sun, G. D., Cui, W. P., Guo, Q. Y., and Miao, L. N. (2014). Histone lysine methylation in diabetic nephropathy. *Diabetes Res.* 2014, 654148. doi:10.1155/2014/654148
- Tong, Z., Han, C., Qiang, M., Wang, W., Lv, J., Zhang, S., et al. (2015). Age-related formaldehyde interferes with DNA methyltransferase function, causing memory loss in Alzheimer's disease. *Neurobiol. Aging* 36, 100–110. doi:10.1016/j.neurobiolaging.2014.07.018

- Tong, Z., Zhang, J., Luo, W., Wang, W., Li, F., Li, H., et al. (2011). Urine formaldehyde level is inversely correlated to mini mental state examination scores in senile dementia. *Neurobiol. Aging* 32, 31–41. doi:10.1016/j.neurobiolaging.2009.07.013
- Tsou, C. L. (1962). Relation between modification of functional groups of proteins and their biological activity. I. A graphical method for the determination of the number and type of essential groups. *Sci. Sin.* 11, 1535–1558.
- Twarda-Clapa, A., Olczak, A., Białkowska, A. M., and Koziolkiewicz, M. (2022). Advanced glycation end-products (AGEs): Formation, chemistry, classification, receptors, and diseases related to AGEs. *Cells* 8, 1312. doi:10.3390/cells11081312
- Walport, L. J., Hopkinson, R. J., and Schofield, C. J. (2012). Mechanisms of human histone and nucleic acid demethylases. *Curr. Opin. Chem. Biol.* 16, 525–534. doi:10.1016/j.cbpa.2012.09.015
- Wang, R., Yu, X., Gkousioudi, A., and Zhang, Y. (2021). Effect of glycation on interlamellar bonding of arterial elastin. *Exp. Mech.* 61, 81–94. doi:10.1007/s11340-020-00644-y
- Wei, Y., Wang, Y.-J., Wu, B.-B., Zhang, Y.-H., and He, R.-Q. (2016). Ribosylated BSA monomer is severely toxic to SH-SY5Y cells. *Prog. Biochem. Biophys.* 43, 579–591. doi:10.16476/j.pibb.2016.0054
- Wu, B., Wang, Y., Shi, C., Chen, Y., Yu, L., Li, J., et al. (2019). Ribosylation-Derived Advanced glycation end products induce tau hyperphosphorylation through brain-derived neurotrophic factor reduction. *J. Alzheimers Dis.* 71, 291–305. doi:10.3233/JAD-190158
- Wu, B., Yu, L., Hu, P., Lu, Y., Li, J., Wei, Y., et al. (2018). GRP78 protects CHO cells from ribosylation. *Biochim. Biophys. Acta. Mol. Cell Res.* 1865, 629–637. doi:10.1016/j.bbamcr.2018.02.001
- Xin, F., Tian, Y., Gao, C., Guo, B., Wu, Y., Zhao, J., et al. (2019). A two-photon fluorescent probe for basal formaldehyde imaging in zebrafish and visualization of mitochondrial damage induced by FA stress. *Analyst* 144, 2297–2303. doi:10.1039/c8an02108b
- Yamunadevi, A., Pratibha, R., Rajmohan, M., Mahendrapurumal, S., and Ganapathy, N. (2021). Basics of epigenetics and role of epigenetics in diabetic complications. *J. Pharm. Bioallied Sci.* 13, S336–S343. doi:10.4103/jpbs.JPBS_771_20
- Yang, C., Xia, L., He, T., Gou, Y., Tang, Y., Peng, X., et al. (2020). The progress of epigenetic modification in hematological malignancies research. *Prog. Biochem. Biophys.* 47, 386–398.
- Yang, Y., Luan, Y., Feng, Q., Chen, X., Qin, B., Ren, K. D., et al. (2022). Epigenetics and beyond: Targeting histone methylation to treat type 2 diabetes mellitus. *Front. Pharmacol.* 12, 807413. doi:10.3389/fphar.2021.807413
- Yu, J., Su, T., Zhou, T., He, Y., Lu, J., Li, J., et al. (2014). Uric formaldehyde levels are negatively correlated with cognitive abilities in healthy older adults. *Neurosci. Bull.* 30, 172–184. doi:10.1007/s12264-013-1416-x
- Yu, L., Chen, Y., Xu, Y., He, T., Wei, Y., and He, R. (2019). D-ribose is elevated in T1DM patients and can be involved in the onset of encephalopathy. *Aging* 11, 4943–4969. doi:10.18632/aging.102089
- Yu, P. H., Lu, L. X., Fan, H., Kazachkov, M., Jiang, Z. J., Jalkanen, S., et al. (2006). Involvement of semicarbazide-sensitive amine oxidase-mediated deamination in lipopolysaccharide-induced pulmonary inflammation. *Am. J. Pathol.* 168, 718–726. doi:10.2353/ajpath.2006.050970
- Zhang, H. B., Zhang, Y., Chen, C., Li, Y. Q., Ma, C., and Wang, Z. J. (2016). Pioglitazone inhibits advanced glycation end product-induced matrix metalloproteinases and apoptosis by suppressing the activation of MAPK and NF- κ B. *Apoptosis* 10, 1082–1093. doi:10.1007/s10495-016-1280-z
- Zhang, L., Meng, C. X., and Zhang, M. W. (2020). Simulation of ship radiated noise field in deep sea based on statistical characteristics of sound source. *Procedia Comput. Sci.* 166, 104–110. doi:10.1016/j.procs.2020.02.029
- Zhang, N., Zhao, S., Hong, J., Li, W., and Wang, X. (2019). Protective effects of Kaempferol on D-ribose-induced mesangial cell injury. *Oxid. Med. Cell. Longev.* 2019, 7564207. doi:10.1155/2019/7564207
- Zheng, Q., Maksimovic, I., Upad, A., and David, Y. (2020a). Non-enzymatic covalent modifications: A new link between metabolism and epigenetics. *Protein Cell* 11, 401–416. doi:10.1007/s13238-020-00722-w
- Zheng, Q., Omans, N. D., Leicher, R., Osunsade, A., Agustinus, A. S., Finkin-Groner, E., et al. (2019). Reversible histone glycation is associated with disease-related changes in chromatin architecture. *Nat. Commun.* 10, 1289. doi:10.1038/s41467-019-09192-z
- Zheng, Q., Osunsade, A., and David, Y. (2020b). Protein arginine deiminase 4 antagonizes methylglyoxal-induced histone glycation. *Nat. Commun.* 11, 3241. doi:10.1038/s41467-020-17066-y
- Zhong, Q., and Kowluru, R. A. (2013). Epigenetic modification of Sod2 in the development of diabetic retinopathy and in the metabolic memory: Role of histone methylation. *Invest. Ophthalmol. Vis. Sci.* 54, 244–250. doi:10.1167/iovs.12-10854